Journal of Power Sources 196 (2011) 9665–9671

Contents lists available at ScienceDirect

Journal of Power Sources

journal homepage: www.elsevier.com/locate/jpowsour

High performance, environmentally friendly and low cost anodes for lithium-ion battery based on TiO_2 anatase and water soluble binder carboxymethyl cellulose

M. Mancini[a,*], F. Nobili[a], R. Tossici[a], M. Wohlfahrt-Mehrens[b], R. Marassi[a]

[a] School of Science and Technology, Chemistry Division, Camerino University, Via S. Agostino 1, I-62032 Camerino, Italy
[b] ZSW-Centre for Solar Energy and Hydrogen Research, Helmholtzstraße 8, D-89081 Ulm, Germany

ARTICLE INFO

Article history:
Received 30 May 2011
Received in revised form 6 July 2011
Accepted 7 July 2011
Available online 19 July 2011

Keywords:
Lithium-ion battery
Binder
Carboxymethyl cellulose (CMC)
Anatase TiO_2

ABSTRACT

The challenge of producing lithium-ion batteries meeting performance requirements and low environmental impact is strictly related to the choice of materials as well as to the manufacturing processes. Most electrodes are currently prepared using poly(vinilydene fluoride) (PVDF) as binder. This fluorinated polymer is expensive and requires the use of a volatile and toxic organic solvent such as N-methyl-pyrrolidone (NMP) in the processing. Water soluble sodium carboxymethyl cellulose (CMC) can be a suitable substitute for PVDF as binder for both anodes and cathodes eliminating the necessity of NMP and thus decreasing the cost and the environmental impact of battery production. In this work, CMC has been successfully used to prepare efficient and stable anatase TiO_2 anodes by optimizing the electrode manufacturing process in terms of composition and compression. The stability and the high rate performances of the TiO_2/CMC are described and compared with those of TiO_2/PVDF electrodes. The compatibility of the TiO_2/CMC with a $LiFePO_4$ cathode in a full-cell is also reported.

1. Introduction

The market request for high energy density rechargeable lithium-ion batteries for applications such as EV and HEV calls for high safety standards and low-cost materials. Moreover, the increase of environment related problems imposes the development of green processes for the batteries production and disposal. Therefore, there is an increasing interest in the development of safer and less toxic electrolytes and electrode materials and in the improvement of electrode fabrication process and components recycling. Electrode composition and engineering are also crucial for battery performances and safety [1]. Beside the use of inherently safe electrode materials (e.g. $LiFePO_4$ and lithium titanates) and electrolyte systems [1,2], the choice of the type and amount of binder in the electrode composition is also very important to optimize electrode cost, energy density, stability and production procedure [1]. Due to its suitable properties in terms of electrochemical stability and adhesion between active material, conductive agents and current collectors, PVDF is at present the most widely used binder for anodes and cathodes preparation. However, the use PVDF in electrode manufacturing requires an organic solvent, such as N-methyl pyrrolidone (NMP) that is expensive, volatile and toxic. Due to environmental hazard, NMP, that evaporates during electrode drying, must be collected and purified with additional costs in the overall production process. It has been also demonstrated that PVDF reacts with metallic lithium and lithiated graphite especially at high temperatures, with the risk of self-heating thermal runaway [1,2]. Recently alternative binders such as water soluble sodium carboxymethyl cellulose (CMC) have been investigated [1–11]. Natural graphite [12], MCMB [13], $Li_4Ti_5O_{12}$ [3], tin and silicon anodes [8,11,14–16] and $LiFePO_4$ cathodes [3,17] using CMC as binders have been reported. The main advantages in using CMC instead of PVDF are related to its lower cost and to the possibility to replace NMP with water during electrode fabrication thus decreasing the cost and the environmental impact of the battery production.

Sodium CMC is a linear polymeric derivative of natural cellulose, made water soluble because of the presence of carboxy-methyl groups. Different levels of carboxy-methyl ($-OCH_2COO^-\ Na^+$) substitution are possible up to the maximum degree of substitution of 3 (DS = 3). It has been demonstrated that CMC, either alone or in combination with styrene butadiene block co-polymer (SBR), can replace PVDF as binder providing good cycleability and mechanical stability to electrodes that suffer of severe volume expansion during cycling (e.g. tin–lithium alloys) [8,18]. CMC as binder in graphite electrodes, in addition, lowers the irreversible capacity loss (ICL) in the first cycle and improves the high rate performances [8].

This paper describes the possible use of CMC binder in TiO_2-based electrodes. Titanium dioxide offers a range of physical and chemical properties that make it suitable for a wide spectrum of

* Corresponding author. Tel.: +39 737 402259; fax: +39 737 402296.
E-mail address: marilena.mancini@unicam.it (M. Mancini).

0378-7753/$ – see front matter © 2011 Elsevier B.V. All rights reserved.
doi:10.1016/j.jpowsour.2011.07.028

applications such as photoelectrochemistry [19], electrochromic devices [20], catalysis [21], gas sensing [22], and dye-sensitised solar cells [23]. Being biocompatible, environmentally friendly and readily available, TiO_2 is also a promising candidate to replace the carbon-based anode material for lithium-ion batteries. Among different TiO_2 polymorphs, anatase presents fast lithium insertion/extraction reactions and high insertion capacity [24–32]. The reversible electrochemical process of lithium insertion into anatase occurs according to the following reaction:

$$TiO_2 + x(Li^+ + e^-) = Li_xTiO_2 \quad (1)$$

where x is the number of lithium ions inserted per mole of TiO_2. The maximum theoretical capacity corresponding to $x = 1$ is 335 mA h g^{-1}. From a practical point of view, the degree of insertion is limited to $x = 0.5$, corresponding to the two-phase equilibrium between the Li-poor $Li_{0.05}TiO_2$ and the Li-rich $Li_{0.5}TiO_2$ phases. The associated reversible capacity is, therefore, 168 mA h g^{-1} [27–29]. Anatase particle size and morphology have a strong influence on lithium insertion ability. It has been demonstrated that the use of nanosized anatase [28,30] results in enhanced kinetics of the lithium insertion/extraction process and higher reversible capacity, with lithium storage capability close to the theoretical value [31,32]. In particular, mesoporous materials are effective in increasing the lithium insertion capacity, especially at high charge/discharge rates [26,33,34]. In order to improve the material conductivity different strategies have been explored including the addition of conductive phases such as carbon, conductive polymers, or metals [25,35–38]. Electrochemical lithium insertion and extraction occur at relatively high voltage vs. Li (about 1.8 V and 2 V, respectively). This means that the energy density of the lithium-ion battery is significantly reduced when a TiO_2 anode replaces the conventional graphite negative electrode. On the other hand, the high working potential of the TiO_2 anode reduces safety problems of the lithium-ion cell that are typically related to the use of graphite. In fact, at these potential values no electrolyte reduction takes place at the electrode surface. As a consequence, SEI formation and high values of irreversible capacity losses (ILC) are avoided. In addition lithium deposition is highly improbable making the batteries much safer than those using graphite anodes.

This paper deals with the electrochemical behavior of TiO_2/CMC electrodes that, to the best of our knowledge, has never been reported. For comparison, electrodes prepared with PVDF binder have been also tested. The electrodes were tested either vs. metallic lithium or in complete cells using $LiFePO_4$ as cathode active material. Important parameters such as density, porosity and binder amount have been considered. The results are discussed in terms of reversible specific capacity, high rate performances and long term stability.

2. Experimental

A commercial nanocrystalline anatase TiO_2 (Hombikat N100, Sachtleben, Germany, particle size (d_{50}) = 2 μm, crystal size = 20 nm, BET surface area = 100 m^2 g^{-1}, density 4.1 g cm^{-3}) was used as active material with Super P carbon (density 2 g cm^{-3}) as conductive agent, sodium carboxymethyl cellulose (CMC, Aldrich, density 1.59 g cm^{-3}) and poly(vinilydene fluoride) (PVDF, Aldrich, density 1.71 g cm^{-3}) as binders.

CMC was used as received to prepare a 5% w/o solution in high purity deionized water. Dried PVDF was used to prepare a 5% w/o solution in anhydrous NM2P (N-methyl-2-pyrrolidinone, Aldrich). The composition of the slurry containing PVDF was TiO_2:Super P:binder = 80:10:10 w/o. Several slurries having different compositions have been prepared with CMC binder with w/o ratios TiO_2:Super P:binder: (i) 80:10:10, (ii) 78:10:12, (iii) 82:10:8 and (iv) 85:10:5. The viscosity of the slurry was adjusted by solvent addition. The slurries were coated onto Al foils current collector (Gelon, China) using the doctor blade technique (thickness 200 μm). Circular electrodes were cut from the foil, pressed and dried (130 °C) under vacuum overnight. The diameter of the electrodes was 9 mm for half-cell tests and 16 mm for full-cell. The loading of active material was in the range 2.54–2.77 mg cm^{-2} for either PVDF or CMC-based layers. The cathode composition for full-cell tests was $LiFePO_4$ (Aleees, Taiwan): Super P:PVDF in a weight ratio of 80:10:10 coated on an Al foil. Electrode morphology was investigated using a Cambridge Stereoscan mod. 360 Scanning Electron Microscope (SEM).

The electrochemical measurements were performed using three-electrode cells assembled in an argon-filled glove box. For half-cell measurements the electrodes were assembled in T-cells with metallic lithium as reference and counter electrodes, and a polypropylene film (Celgard 2400) as separator. Full-cells were assembled using coin cells (EL-CELL, Germany) with metallic lithium as reference and a glass fiber (EL-CELL, Germany) as separator. The electrolyte was a 1 M solution of $LiPF_6$ in EC:DMC 1:1 (Merck). All the measurements were carried out at room temperature using a VMP2/Z electrochemical workstation by BioLogic Science Instruments. All potentials are given vs. Li^+/Li. The active material loading ratio cathode/anode for full-cell experiments was about 1.4. For full-cell tests separated control of the anode and cathode potential cut-off were used in order to avoid overcharge or overdischarge of both electrodes. The potential windows were set as 1–3.2 V for the complete cell, 2–4.2 V for the cathode and 1–3 V for the anode. The charge/discharge rates are computed assuming 1 C = 0.168 A g^{-1} as anode theoretical capacity.

3. Results and discussion

3.1. Morphological characterization

The morphology of the electrodes obtained using organic or aqueous processing was probed by Scanning Electron Microscopy (SEM). The SEM analysis has been carried out on electrodes as obtained after drying and before pressing. Fig. 1 shows micrographs of electrodes containing PVDF 10% (a and c) and CMC 10% (b and d), respectively, at different magnifications. The layers prepared with CMC appear more uniform and compact than those prepared with PVDF. The higher electrode compactness is also indicated by the wet/dried thickness layer ratio that was 4:1 (wet = 200 μm; dry = 50 μm) for the PVDF-based layer and 5:1 (wet = 200 μm; dry = 40 μm) for the CMC-based layer. Similar results, not shown for sake of brevity, have been obtained for electrodes with different binder amounts. The result is consistent with those reported in [3] for CMC/$Li_4Ti_5O_{12}$ anodes, where the high compactness of CMC based electrodes has been attributed to the substantial shrinkage of cellulose during the drying step.

3.2. Optimization of CMC content

An important aspect in electrode fabrication is the loading of active material that should be maximized in order to increase the energy density per unit electrode area. The active material mass fraction in the electrode is limited by the amount of conductive and binder additives necessary to optimize electrode stability and conductivity. In order to determine the best active material/binder ratio in the preparation of TiO_2/CMC electrodes, different electrode compositions with amounts of CMC from 5 to 12% w/o have been prepared and tested by galvanostatic charge/discharge cycles at rates ranging 2–8 C. The experiments were performed using electrodes pressed at 0.1 tons cm^{-2} (see Section 3.3). Fig. 2

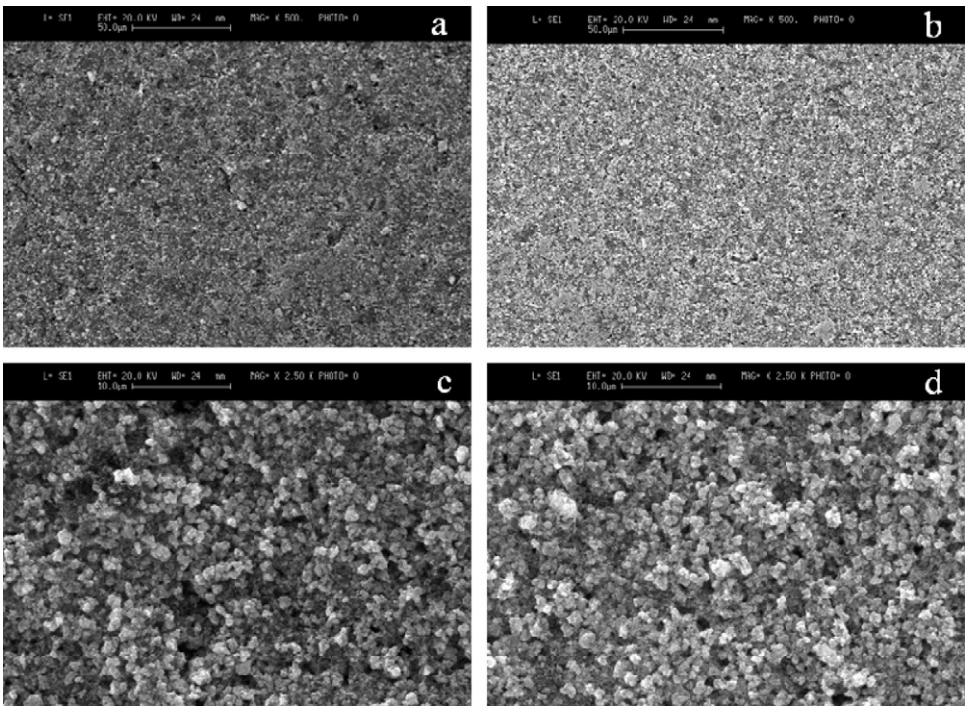

Fig. 1. SEM images of the electrode containing PVDF 10% at magnification levels 500× (a) and 2500× (c) and CMC 10% at 500× (b) and 2500× (d). The images refer to un-pressed electrodes.

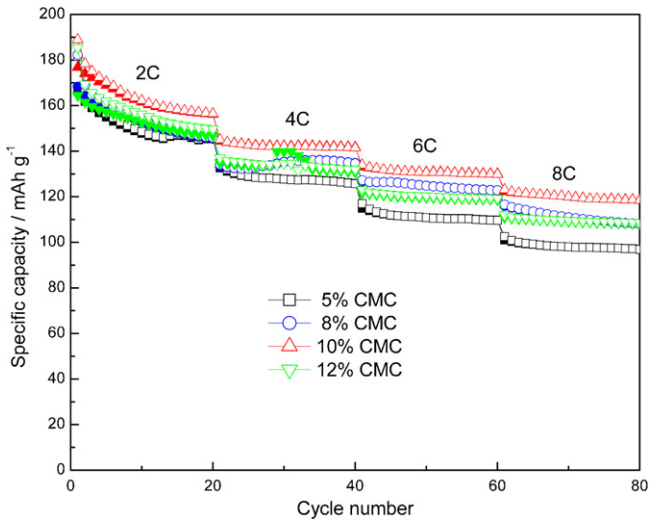

Fig. 2. Lithium insertion (hollow symbols) and extraction (filled symbols) capacities at 2, 4, 6 and 8 C in the potential range 1.2–3 V for TiO_2 electrodes containing different amounts of CMC.

shows the delivered charge/discharge capacities at the different rates. The capacity values averaged over 20 cycles are summarized in Table 1. Regardless of the CMC content, all electrodes show remarkable reversible capacity values and stability upon cycling. However, the electrodes with 10% binder content show the best performances. Based on these results, the electrode formulation TiO_2:Super P:binder 80:10:10 w/o for both CMC and PVDF based electrodes was chosen for further tests.

3.3. *CMC/TiO_2 vs. PVDF/TiO_2 electrodes: effect of the compression pressure*

Electrode pressing is in general necessary to obtain good mechanical contact between TiO_2 and carbon particles and between the layer and the current collector. During this step the electrode thickness and porosity is also optimized. The CMC/TiO_2 and PVDF/TiO_2 electrodes were pressed at 0.1 and 6 tons cm^{-2}. Based on the measured thickness and mass of the electrodes, the apparent electrode densities and porosities have been estimated according to the procedure reported in [39]. For sake of brevity, the un-pressed, pressed at 0.1 and 6 tons cm^{-2} CMC/TiO_2 electrodes are indicated as A, B and C, respectively. The corresponding PVDF/TiO_2 electrodes are indicated as D, E and F. Table 2 summarizes electrode names, calculated densities and porosities values [39]. It is worth to point out that the density values for the un-pressed electrodes, A and D, indirectly confirm that CMC leads to more compact electrodes than PVDF, as already revealed by the SEM micrographs. The effect of the different preparation parameters was evaluated by galvanostatic cycles at increasing charge/discharge rates from 2 C to 8 C. A comparison of the specific discharge capacities obtained for the different electrodes is reported in Fig. 3(a). Electrodes B and F show similar cycling behavior, with good capacity and stability up to 8 C rate; electrode C is also stable upon cycling but the delivered

Table 1
Values of specific discharge capacity averaged on 20 cycles at any current rate.

CMC content (%)	Discharge capacity/mA h g^{-1} 2 C-rate	Discharge capacity/mA h g^{-1} 4 C-rate	Discharge capacity/mA h g^{-1} 6 C-rate	Discharge capacity/mA h g^{-1} 8 C-rate
5%	152.4	128.2	111.4	98.5
8%	152.6	134.5	124.8	111.3
10%	164.7	142.4	131.0	120.1
12%	157.9	134.0	120.5	109.8

Table 2
Apparent density (measured from the thickness of the electrode before and after pressing) and estimated porosity of the different electrodes.

Applied pressure/tons cm^{-2}	Electrode name	Electrode density/g cm^{-3}	Electrode porosity (%)	Type of binder (10%)
0	A	0.79	75.7	CMC
0.1	B	0.83	74.4	CMC
6	C	1.26	61.1	CMC
0	D	0.69	79.0	PVDF
0.1	E	0.87	73.7	PVDF
6	F	1.16	65.0	PVDF

capacities are lower than those of electrodes B and F. Electrode E rapidly loses capacity and stability. The results clearly suggest that the pressure is crucial for PVDF/TiO_2 electrodes, which show good stability when pressed at 6 tons cm^{-2} (F). A lower compression is ineffective in providing suitable compactness, and results in a rapid loss of capacity especially at the highest cycling rates (E). The behavior of the electrodes prepared with CMC is less affected by the applied pressure. The electrodes treated at lower pressure show better performances in terms of reversible capacity and cycling stability. This result is again in agreement with the conclusion in [3] for CMC/$Li_4Ti_5O_{12}$ electrodes, whose compactness may lead to the elimination of a roll-pressing step in the production line with consequent cost and time reduction. The use of CMC also affects the irreversible capacity loss (ICL) in the first cycle (Fig. 3(b)). CMC/TiO_2 electrodes show ICL values in the range 12–13 mA h g^{-1} vs. an average value of 20–25 mA h g^{-1} for the PVDF/TiO_2 electrodes.

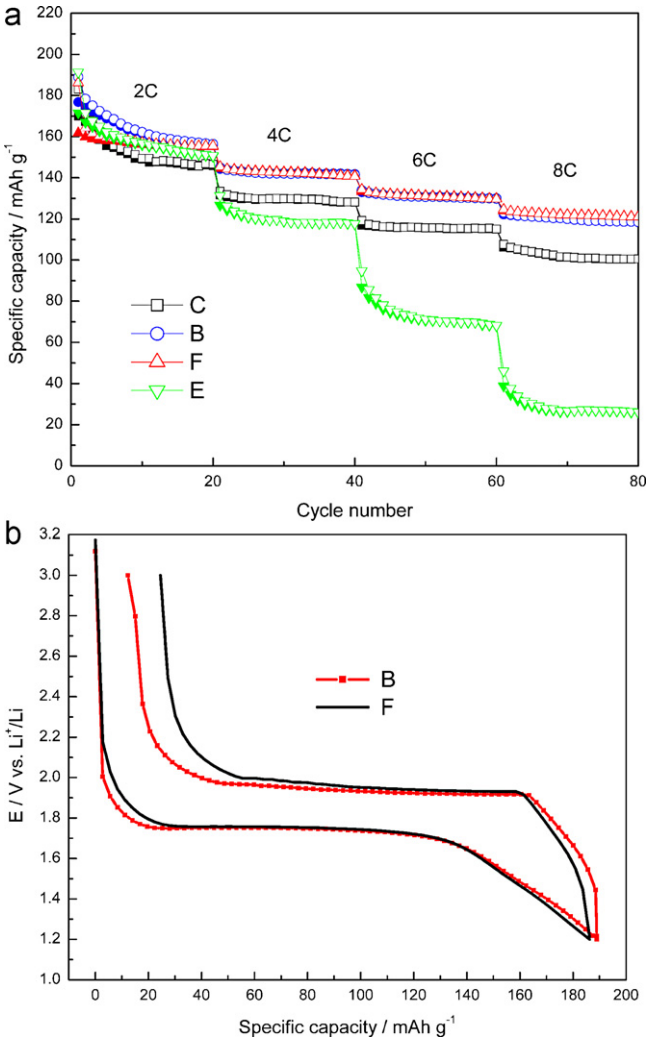

Fig. 3. (a) Comparison between specific lithium insertion (hollow symbols) and extraction (filled symbols) capacities at 2, 4, 6 and 8 C in the potential range 1.2–3 V for CMC and PVDF-based TiO_2 electrodes pressed at different pressures. (b) Comparison between galvanostatic curves of the first cycle (2 C rate) for the electrodes B and F.

The high-rate performances of the different electrodes have been evaluated by galvanostatic cycles at increasing charge/discharge rate ranging C/2 (ca. 0.084 A g^{-1})–30 C (ca. 5.025 A g^{-1}). Fig. 4(a–d) shows the lithium insertion profiles of the different electrodes recorded at 0.5 C, 5 C, 15 C and 20 C, respectively. Fig. 5 summarizes the capacities of the different electrodes as a function of the charge/discharge rate. At low rates, i.e. 0.5 C, the voltage profiles are very similar for all electrodes, with charge capacity values close to 185 mA h g^{-1} (Fig. 4(a)). When the charge/discharge rate is increased, electrode E rapidly loses its capacity, and at 20 C the plateau disappears (Fig. 4(d)). The electrode made with CMC and pressed at 0.1 tons cm^{-2} (electrode B) shows the best performances. Electrode C (CMC/TiO_2, 6 tons cm^{-2}) shows higher polarization and lower capacity than electrode B. Nevertheless, it still reaches specific capacity values close to 65 mA h g^{-1} at 30 C. These results confirm that replacing PVDF with CMC in anatase-based electrode leads to more compact layers and better electrochemical performances without the need of applying high pressures.

3.4. Stability and full-cell experiments

All the previous galvanostatic experiments have been performed by cycling the electrodes in the potential range 1.2–3 V. It is known that for anatase electrodes the lower cut-off can be reduced from 1.2 V to 1 V, resulting in an increased capacity due to capacitive contributions [26,27,30], generally at the expenses of a decreased stability. On the other hand, the increase of the working potential window of the TiO_2 anodes is important to design a complete cell with suitable energy density. For this reason, the long-term stability of electrodes containing 5, 8 or 10% w/o CMC has been tested by galvanostatic cycles in the potential range 1–3 V at a constant rate of 5 C. Fig. 6 shows the variation of the capacity during 200 cycles. Some small variation in long-term capacity is due to ambient temperature changes during the experiment.

The first cycle insertion capacity values range 170–180 mA h g^{-1} with ICL in the first cycle between 15 and 19 mA h g^{-1}. During the initial cycles the specific capacity decreases rather rapidly down to about 125 mA h g^{-1}. This is probably due to "stabilization" effects of the electrode upon cycling, that include interactions at the interface between active material and electrolyte, related to the low porosity and to the hydrophilic properties of the CMC/TiO_2 electrodes, as well as processes of topotactic lithium insertion in the anatase surface layers that are known to occur at potentials below 1.7 V [26]. The overall effect is that several cycles are necessary to reach a stable value of specific capacity.

However, while for electrodes containing 5 and 8% CMC the decrease in capacity continues upon cycling, the capacity of the electrodes containing 10% CMC, after the initial decrease, increases to the stable value of about 140 mA h g^{-1}. For this electrode, a capacity retention of 83.7% is observed after 200 cycles. The reasons of this behavior are at present not completely understood and will be

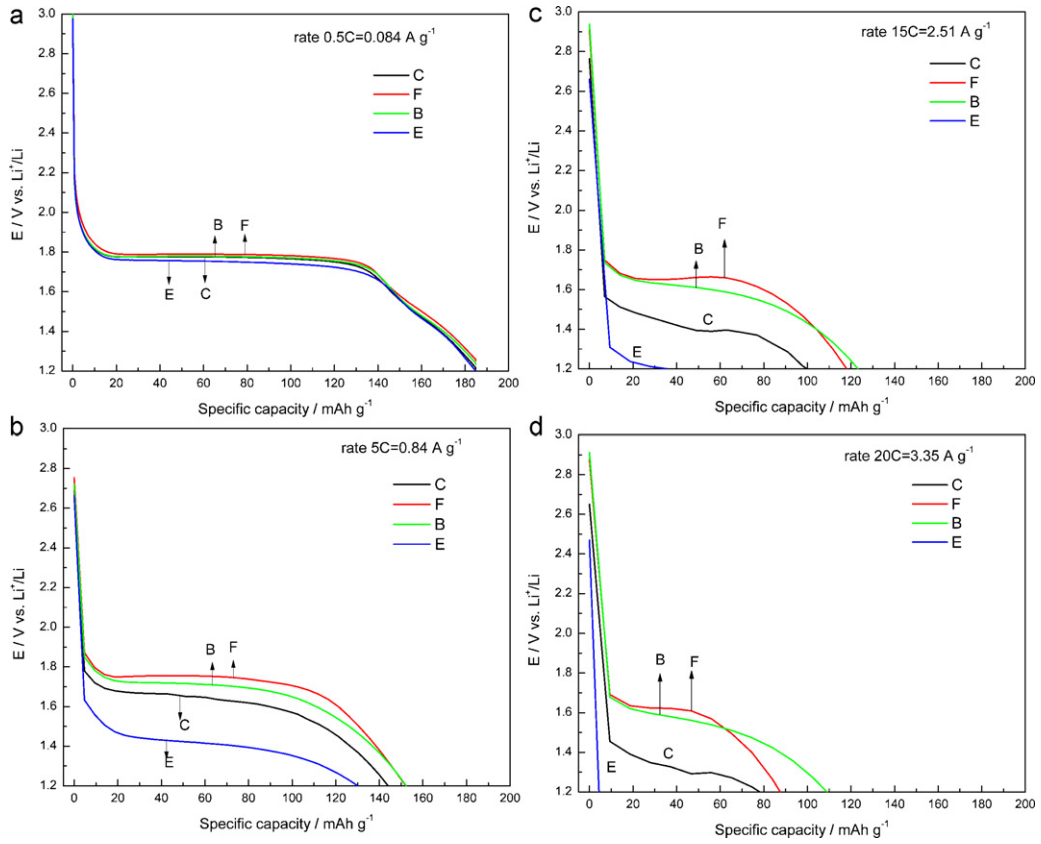

Fig. 4. Galvanostatic lithium insertion curves at rates 0.5 C (a), 5 C (b), 15 C (c), 20 C (d), for the CMC- and PVDF-based TiO_2 electrodes pressed at different pressures. Potential range 1.2–3 V.

the subject of further studies. A probable reason is an increase of electrode wettability and electrolyte penetration.

These results show that, for the electrodes with 10% CMC, the low potential cut-off can be reduced, thus expanding the potential window and increasing the energy density for the full-cell, without affecting anode capacity and stability. The compatibility of this kind of anodes with a commercial cathode has been demonstrated by assembling a battery with a $LiFePO_4$ cathode. The full-cell was tested in the potential range 1–3.2 V at 1 C. The C rate was calculated on the basis of the weight of the anode that was the limiting electrode.

Fig. 7(a) shows the evolution of the capacity and of the coulombic efficiency of the full-cell. The capacity is very stable and the columbic efficiency closes to 100%. The cell delivers about 0.775 mA h, which corresponds, based on the active material weight, to 150 mA h g^{-1} for the anode and 110 mA h g^{-1} for the cathode. Fig. 7(b) shows the charge voltage profiles of the full-cell at some selected cycles. Changes in cell potential profile, with a

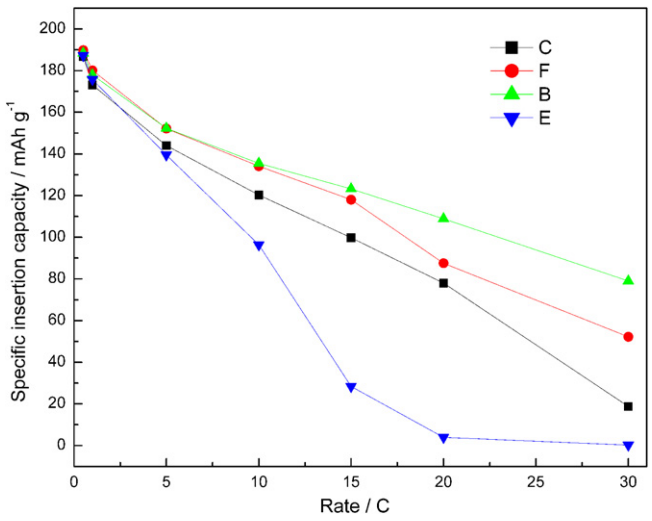

Fig. 5. Reversible capacity vs. charge/discharge rate of the CMC- and PVDF-based TiO_2 electrodes pressed at different pressures. Potential range 1.2–3 V.

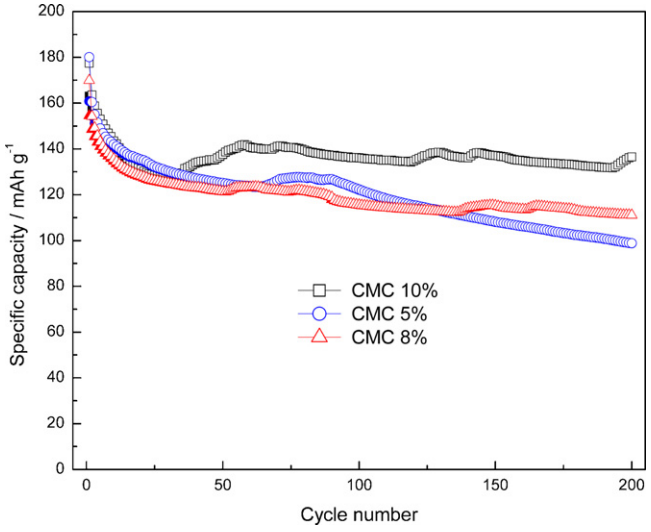

Fig. 6. Comparison between specific charge/discharge capacities at 5 C in the potential range 1–3 V for TiO_2 electrodes containing different amounts of CMC.

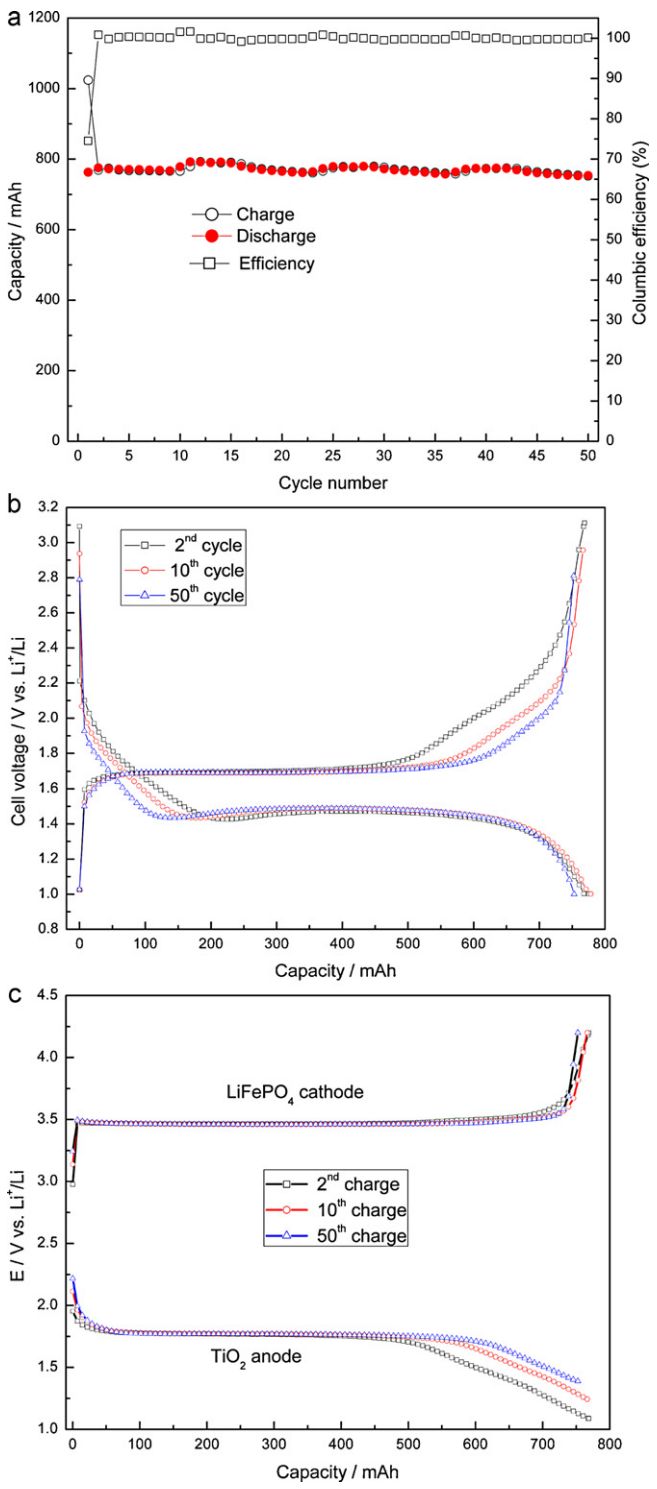

Fig. 7. (a) Cycling performances of the full-cell made with TiO_2/CMC anode and $LiFePO_4$ cathode at 1 C charge/discharge rate. (b) Charge and discharge voltage profiles at selected cycles of the full-cell and (c) related charge profiles of TiO_2/CMC anode and $LiFePO_4$ cathode.

plateau length increase, occur upon cycling. This is due to a progressive increase of the anode capacity, as observed in Fig. 7(c) that shows the corresponding voltage profiles, vs. Li reference, of both anode and cathode. According to the results shown in Fig. 6, the TiO_2/CMC anode needs several cycles to reach the maximum capacity, therefore a higher cathode/anode mass ratio is necessary for a correct balance of the full-cell. However, the results demonstrate that TiO_2 anodes in which PVDF is replaced by CMC are compatible with $LiFePO_4$ cathode. Further studies on the properties of the TiO_2/CMC electrodes, including electrode kinetics and optimization of full-cell balance, will be the subject of a further publication.

4. Conclusions

The use of non toxic, cheap and readily available materials such us anatase TiO_2 and CMC to prepare electrodes combining a green manufacturing process and high performances is a very promising strategy for the optimization of large-scale production of lithium-ion batteries. The present work demonstrates that CMC can be used as binder for the preparation of anatase TiO_2 electrodes using an aqueous process and reducing the environmental related problems during production and disposal. The CMC/TiO_2 electrodes show, in addition, more compactness and better electrochemical behavior than those containing PVDF as binder. This is probably due to different interactions between the binder, the active material and carbon that translate into suitable properties in terms of porosity, wettability and compactness of the composite electrodes. Another advantage in large-scale electrode manufacturing is that the pressing step is less crucial, or even not necessary. In conclusion, the advantages of using CMC instead PVDF for TiO_2 anodes for lithium-ion batteries are: (i) replacement of toxic and volatile organic solvents with water during electrode manufacturing; (ii) more compact layers with porosity close to the optimum value and consequent less critical pressing process during electrode preparation; (iii) better electrode capacity at high charge/discharge rates; (iv) lower irreversible capacity loss.

Acknowledgements

Support by ENI under the contract LiBEST is acknowledged. Sachtleben Chemie GmbH is acknowledged for supplying the anatase sample.

References

[1] X. Zhang, P.N. Ross, R. Kostecki, F. Kong, S. Sloop, J.B. Kerr, K. Striebel, E.J. Cairns, F. McLarnon, J. Electrochem. Soc. 148 (2001) A463.
[2] L. Damen, J. Hassoun, M. Mastragostino, B. Scrosati, J. Power Sources 195 (2010) 6902.
[3] G.T. Kim, S.S. Jeong, M. Joost, E. Rocca, M. Winter, S. Passerini, A. Balducci, J. Power Sources 196 (2011) 2187.
[4] L. Fransson, T. Eriksson, K. Edström, T. Gustafsson, J.O. Thomas, J. Power Sources 101 (2001) 1.
[5] E.P. Roth, D.H. Doughty, J. Franklin, J. Power Sources 134 (2004) 222.
[6] H. Maleki, G. Deng, I. Kerzhner-Haller, A. Anani, J.N. Howard, J. Electrochem. Soc. 147 (12) (2000) 4470.
[7] S.S. Zhang, K. Xu, T.R. Jow, J. Power Sources 138 (2004) 226.
[8] H. Buqa, M. Holzapfel, F. Krumeich, C. Veit, P. Novák, J. Power Sources 161 (1) (2006) 617.
[9] A. Guerfi, M. Kaneko, M. Petitclerc, M. Mori, K. Zaghib, J. Power Sources 163 (2007) 1047.
[10] D. Guy, B. Lestriez, R. Bouchet, V. Gaudefroy, D. Guyomard, J. Power Sources 157 (2006) 438.
[11] N.S. Hochgatterer, M.R. Schweiger, S. Koller, P.R. Raimann, T. Wohrle, C. Wurm, M. Winter, Electrochem. Solid-State Lett. 11 (5) (2008) A76.
[12] J.-H. Lee, U. Paik, V.A. Hackley, Y.-M. Choi, J. Electrochem. Soc. 152 (9) (2005) A1763.
[13] F.M. Courtel, S. Niketic, D. Duguay, Y. Abu-Lebdeh, I.J. Davidson, J. Power Sources 196 (2011) 2128.
[14] J. Li, R.B. Lewis, J.R. Dahn, Electrochem. Solid-State Lett. 10 (2) (2007) A17.
[15] S.D. Beattie, D. Larcher, M. Morcrette, B. Simon, J.M. Tarascon, J. Electrochem. Soc. 155 (2) (2008) A158.
[16] W.-R. Liu, M.-H. Yang, H.-C. Wu, S.M. Chiao, N.-L. Wu, Electrochem. Solid-State Lett. 8 (2) (2005) A100.
[17] S.F. Lux, F. Schappacher, A. Balducci, S. Passerini, M. Winter, J. Electrochem. Soc. 157 (3) (2010) A320.
[18] L. Noerochim, J.Z. Wang, S.L. Chou, H.J. Li, H.K. Liu, Electrochim. Acta 56 (2010) 314–320.
[19] Y. Xie, Electrochim. Acta 51 (2006) 3399.
[20] A. Hagfeldt, N. Vlachopolous, M. Grätzel, J. Electrochem. Soc. 141 (1994) L82.
[21] D. Li, H. Haneda, S. Hishita, N. Ohashi, Chem. Mater. 17 (2005) 2596.

[22] Y. Lei, L.D. Zhang, J.C. Fan, Chem. Phys. Lett. 338 (2001) 231.
[23] G.E. Tulloch, J. Photochem. Photobiol. A: Chem. 164 (2004) 209.
[24] Z. Yang, D. Choi, S. Kerisit, K.M. Rosso, D. Wang, J. Zhang, G. Graff, J. Liu, J. Power Sources 192 (2009) 588.
[25] M. Mancini, P. Kubiak, J. Geserick, R. Marassi, N. Hüsing, M. Wohlfahrt-Mehrens, J. Power Sources 189 (2009) 585.
[26] P. Kubiak, J. Geserick, N. Hüsing, M. Wohlfahrt-Mehrens, J. Power Sources 175 (2008) 510.
[27] C. Jiang, M. Wei, Z. Qi, T. Kudo, I. Honma, H. Zhou, J. Power Sources 166 (2007) 239.
[28] S. Huang, L. Kavan, I. Exnar, M. Grätzel, J. Electrochem. Soc. 142 (1995) L142.
[29] R. Baddour-Hadjean, S. Bach, M. Smirnov, J.-P. Pereira-Ramos, J. Raman Spectrosc. 35 (2004) 577.
[30] L. Kavan, M. Kalbac, M. Zukalova, I. Exnar, V. Lorenzen, R. Nesper, M. Grätzel, Chem. Mater. 16 (2004) 477.
[31] J. Wang, J. Polleux, J. Lim, B. Dunn, J. Phys. Chem. C 111 (2007) 14925.
[32] M. Wagemaker, W.J.H. Borghols, F.M. Mulder, J. Am. Chem. Soc. 129 (2007) 4323.
[33] Y.G. Guo, Y.S. Hu, J. Maier, Chem. Commun. 26 (2006) 2783.
[34] D. Fatthakova, M. Wark, T. Brezesinski, B. Smarsly, J. Rathousky, Adv. Funct. Mater. 19 (2007) 2087.
[35] Y.G. Guo, Y.S. Hu, W. Sigle, J. Maier, Adv. Mater. 19 (2007) 2087.
[36] I. Moriguchi, R. Hidaka, H. Yamada, T. Kudo, H. Murakami, N. Nakashima, Adv. Mater. 18 (2006) 69.
[37] M. Mancini, P. Kubiak, M. Wohlfahrt-Mehrens, R. Marassi, J. Electrochem. Soc. 157 (2) (2010) A164.
[38] D. Wang, D. Choi, J. Li, Z. Yang, Z. Nie, R. Kou, D. Hu, C. Wang, L.V. Saraf, J. Zhang, I.A. Aksay, J. Liu, ACS Nano 3 (4) (2009) 907.
[39] T. Marks, S. Trussler, A.J. Smith, D. Xiong, J.R. Dahn, J. Electrochem. Soc. 158 (1) (2011) A51.